PHYSICAL REVIEW D **90,** 014502 (2014)

$D^0 - \bar{D}^0$ mixing in the standard model and beyond from $N_f = 2$ twisted mass QCD

N. Carrasco,[1] M. Ciuchini,[1] P. Dimopoulos,[3,4] R. Frezzotti,[3,5] V. Gimenez,[6] V. Lubicz,[1,2] G. C. Rossi,[3,5] F. Sanfilippo,[8] L. Silvestrini,[7] S. Simula,[1] and C. Tarantino[1,2]

[1]*INFN, Sezione di Roma Tre, Via della Vasca Navale 84, I-00146 Rome, Italy*
[2]*Dipartimento di Matematica e Fisica, Università Roma Tre, Via della Vasca Navale 84, I-00146 Rome, Italy*
[3]*Dipartimento di Fisica, Università di Roma "Tor Vergata," Via della Ricerca Scientifica 1, I-00133 Rome, Italy*
[4]*Centro Fermi-Museo Storico della Fisica e Centro Studi e Ricerche Enrico Fermi, Compendio del Viminale, Piazza del Viminale 1, I-00184 Rome, Italy*
[5]*INFN, Sezione di "Tor Vergata," Via della Ricerca Scientifica 1, I-00133 Rome, Italy*
[6]*Departament de Física Teòrica and IFIC, Universitat de València-CSIC Dr. Moliner 50, E-46100 València, Spain*
[7]*INFN, Sezione di Roma, Piazzale A. Moro, I-00185 Rome, Italy*
[8]*School of Physics and Astronomy, University of Southampton, SO17 1BJ Southampton, United Kingdom*

(Received 16 April 2014; published 3 July 2014)

We present the first unquenched lattice QCD results for the bag parameters controlling the short distance contribution to D meson oscillations in the standard model and beyond. We have used the gauge configurations produced by the European Twisted Mass collaboration with $N_f = 2$ dynamical quarks, at four lattice spacings and light meson masses in the range 280–500 MeV. Renormalization is carried out nonperturbatively with the regularization-independent momentum subtraction method. The bag-parameter results have been used to constrain new physics effects in $D^0 - \bar{D}^0$ mixing, to put a lower bound to the generic new physics scale and to constrain off-diagonal squark mass terms for TeV-scale supersymmetry.

DOI: 10.1103/PhysRevD.90.014502 PACS numbers: 12.38.Gc, 12.60.-i, 14.40.Lb

I. INTRODUCTION

The study of meson oscillations currently represents one of the most powerful probes in searching for new physics (NP). The K and $B_{(s)}$ systems are well studied experimentally and all the available data are compatible with the standard model (SM) predictions. Improved theoretical predictions and future experiments will be important to look for possible NP effects with higher accuracy. The phenomenon of $D^0 - \bar{D}^0$ mixing has been established only in 2007 [1,2]. As it involves mesons with up-type quarks, it is complementary to K and $B_{(s)}$ oscillations in providing information on NP. From the theory side, $D^0 - \bar{D}^0$ mixing has the disadvantage of being affected by large long-distance effects, related to the down and strange quarks circulating in the box diagrams. Only order of magnitude estimates exist for the long-distance contributions and they are at the level of the experimental constraints. However, the SM contribution to $D^0 - \bar{D}^0$ mixing is real to very high accuracy. Therefore, in spite of the SM uncertainty, significant constraints on NP can be obtained in this sector from CP-violating observables [3–22]. These constraints rely on the lattice computation of the bag parameters of four-fermion operators describing $D^0 - \bar{D}^0$ mixing beyond the SM.

In this paper we use the $N_f = 2$ gauge configurations [23,24], generated by the European Twisted Mass collaboration (ETMC), at four values of the lattice spacing to obtain continuum limit estimates for the full basis of $\Delta C = 2$ four-fermion operators. This is the first unquenched calculation of the whole set of D meson bag parameters.

The most general $\Delta C = 2$ effective Hamiltonian of dimension-six operators is

$$H_{\rm eff}^{\Delta C=2} = \frac{1}{4}\sum_{i=1}^{5} C_i(\mu) Q_i(\mu), \tag{1}$$

where μ is the renormalization scale and C_i are the model-dependent Wilson coefficients encoding the short distance contributions. The operators Q_i involving light (ℓ) and charm (c) quarks read, in the so-called SUSY basis,

$$\begin{aligned}
Q_1 &= [\bar{c}^a \gamma_\mu (1-\gamma_5) \ell^a][\bar{c}^b \gamma_\mu (1-\gamma_5) \ell^b], \\
Q_2 &= [\bar{c}^a (1-\gamma_5) \ell^a][\bar{c}^b (1-\gamma_5) \ell^b], \\
Q_3 &= [\bar{c}^a (1-\gamma_5) \ell^b][\bar{c}^b (1-\gamma_5) \ell^a], \\
Q_4 &= [\bar{c}^a (1-\gamma_5) \ell^a][\bar{c}^b (1+\gamma_5) \ell^b], \\
Q_5 &= [\bar{c}^a (1-\gamma_5) \ell^b][\bar{c}^b (1+\gamma_5) \ell^a],
\end{aligned} \tag{2}$$

where a, b are color indices and Dirac indices (understood) are contracted within brackets. In the SM only Q_1 enters the effective Hamiltonian.

TABLE I. Results for the bag parameters of $\bar{D}^0 - D^0$ mixing, renormalized in the $\overline{\rm MS}$ scheme of Ref. [26] and in the regularization-independent momentum subtraction (RI-MOM) scheme at 3 GeV.

	B_1	B_2	B_3	B_4	B_5
$\overline{\rm MS}$ (3 GeV)	0.75(02)	0.66(02)	0.96(05)	0.91(04)	1.10(05)
RI-MOM (3 GeV)	0.74(02)	0.82(03)	1.21(06)	1.09(05)	1.35(06)

According to the operator product expansion, the long-distance nonperturbative QCD contributions are enclosed in the matrix elements of the renormalized four-fermion operators, which can be written in terms of bag parameters as

$$\langle \bar{D}^0|Q_1(\mu)|D^0\rangle = \xi_1 B_1(\mu) m_D^2 f_D^2,$$
$$\langle \bar{D}^0|Q_i(\mu)|D^0\rangle = \xi_i B_i(\mu)\left[\frac{m_D^2 f_D}{\mu_c(\mu)+\mu_\ell(\mu)}\right]^2, \quad \text{for } i = 2, \ldots, 5, \tag{3}$$

where $\xi_i = \{8/3, -5/3, 1/3, 2, 2/3\}$.

For the reader's convenience we give in Table I our final results for the B_i bag parameters, quoting the total uncertainty (statistical and systematic added in quadrature). From these results one notices moderate deviations from the vacuum insertion approximation (the size of which is, of course, scheme dependent) which are much smaller than in the kaon system but larger than for B mesons [25].

As in our recent works on K and $B_{(s)}$ mixing [27,28], we use the results obtained for the full set of $\Delta C = 2$ bag parameters to improve the bounds on the NP scale coming from D-meson mixing, following the method of Ref. [10]. We also recompute the bounds on off-diagonal squark masses from gluino-mediated contributions to $D^0 - \bar{D}^0$ mixing in the minimal supersymmetric standard model (MSSM), updating the analysis presented in Ref. [5]. As for the experimental results we use the recent average of D-meson mixing data computed by the UTfit collaboration [29].

The plan of the paper is as follows. In Sec. II, based on the results of this work for the $\Delta C = 2$ bag parameters, we discuss the bounds coming from D-meson mixing on the NP scale and on off-diagonal squark mass terms. In Sec. III we give details about the lattice simulation and we describe the techniques that have been used in this paper. In Sec. IV we discuss the continuum and chiral extrapolation and we present the results for the bag parameters of the full four-fermion operator basis. We collect in the Appendix the lattice bare bag parameters for all the quark mass combinations and β values we had available.

II. BOUNDS ON THE NP SCALE AND ON THE SQUARK MASS TERMS

$\Delta F = 2$ processes provide some of the most stringent constraints on NP generalizations of the SM. Several phenomenological analyses of $\Delta F = 2$ processes have been performed in the past years, both for specific models and in model-independent frameworks [10,27,30–38]. While the SM prediction for $B^0_{(s)} - \bar{B}^0_{(s)}$ mixing and ε_K is theoretically well under control, the SM contribution to $D^0 - \bar{D}^0$ mixing is plagued by long-distance contributions. However, due to the SM flavor structure, CP violation in $D^0 - \bar{D}^0$ mixing receives negligible SM contributions. Therefore, significant constraints on NP can be obtained in this sector from CP-violating observables.

In two previous papers [27,28] we have presented the first unquenched ($N_f = 2$) lattice QCD results in the continuum limit for the matrix elements of the operators describing K and $B_{(s)}$ oscillations in extensions of the SM. In the same papers we have updated the generalization of the unitarity triangle analysis including possible NP effects, improving the bounds coming from $K^0 - \bar{K}^0$ and $B^0_{(s)} - \bar{B}^0_{(s)}$ mixings.

In a similar way, we present here the first unquenched ($N_f = 2$) lattice QCD results for the bag parameters of the full $\Delta C = 2$ four-fermion operators basis and we use them to improve the bounds coming from D-meson mixing on the NP scale and on the off-diagonal squark mass terms, updating the analysis in Refs. [5,10]. As for the experimental results, we use the recent averages of D-meson mixing data derived by the UTfit collaboration [29]. With the latest experimental updates, the imaginary part of the D mixing amplitude is very strongly constrained, leading to very tight bounds on possible CP-violating NP contributions to the mixing, as shown in Table II.

Let us first discuss the model-independent analysis. The most general effective weak Hamiltonian for D mixing of dimension-six operators is parametrized by Wilson coefficients of the form

$$C_i(\Lambda) = \frac{F_i L_i}{\Lambda^2}, \quad i = 1, \ldots, 5, \tag{4}$$

where F_i is the (generally complex) relevant NP flavor coupling, L_i is a (loop) factor which depends on the interactions that generate $C_i(\Lambda)$, and Λ is the NP scale, i.e. the typical mass of new particles mediating $\Delta C = 2$

TABLE II. 95% probability intervals for the imaginary part of the Wilson coefficients, $\mathrm{Im}C_i^D$, and the corresponding lower bounds on the NP scale, Λ, for a generic strongly interacting NP with generic flavor structure ($L_i = F_i = 1$).

	95% upper limit (GeV^2)	Lower limit on Λ (TeV)
$\mathrm{Im}C_1^D$	$[-0.9, 2.5] \times 10^{-14}$	6.3×10^3
$\mathrm{Im}C_2^D$	$[-2.8, 1.0] \times 10^{-15}$	1.9×10^4
$\mathrm{Im}C_3^D$	$[-3.0, 8.6] \times 10^{-14}$	3.4×10^3
$\mathrm{Im}C_4^D$	$[-2.7, 8.0] \times 10^{-16}$	3.5×10^4
$\mathrm{Im}C_5^D$	$[-0.4, 1.1] \times 10^{-14}$	9.5×10^3

transitions. For a generic strongly interacting theory with an unconstrained flavor structure, one expects $F_i \sim L_i \sim 1$, so that the phenomenologically allowed range for each of the Wilson coefficients can be immediately translated into a lower bound on Λ. Specific assumptions on the flavor structure of NP correspond to special choices of the F_i functions.

Following Ref. [10], in deriving the lower bounds on the NP scale Λ, we assume $L_i = 1$, which corresponds to strongly interacting and/or tree-level coupled NP. Two other interesting possibilities are given by loop-mediated NP contributions proportional to either α_s^2 or α_W^2. The first case corresponds for example to gluino exchange in the MSSM. The second case applies to all models with SM-like loop-mediated weak interactions. To obtain the lower bound on Λ entailed by loop-mediated contributions, one simply has to multiply the bounds we quote in the following by $\alpha_s(\Lambda) \sim 0.1$ or $\alpha_W \sim 0.03$.

The results for the upper bounds on the imaginary part of the Wilson coefficients, $\mathrm{Im}C_i^D$, and the corresponding lower bounds on the NP scale Λ are collected in Table II. The latter are also shown in Fig. 1. The superscript D is to recall that we are reporting the bounds coming from the D-meson sector we are here analyzing.

We remind the reader that the analysis is performed (as in Ref. [10]) by switching on one coefficient at the time in

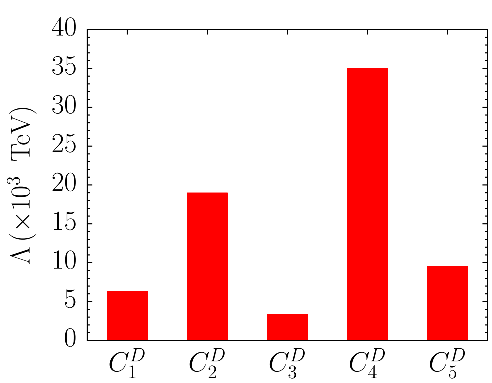

FIG. 1 (color online). Lower bounds on the NP scale as obtained from the constraints on the imaginary part of the Wilson coefficients, $\mathrm{Im}C_i^D$.

each sector, thus barring the possibility of accidental cancellations among the contributions of different operators. Therefore, the reader should keep in mind that the bounds may be weakened if, instead, some accidental cancellation occurs.

In comparison with the analyses in Refs. [27,28], we confirm that the most stringent constraints on the NP scale come from the $K^0 - \bar{K}^0$ matrix elements, while the bounds coming from $D^0 - \bar{D}^0$ are more stringent than those coming from $B^0 - \bar{B}^0$.

We now turn to supersymmetry (SUSY), and consider a general MSSM with arbitrary off-diagonal squark mass terms. In this framework the dominant contribution to flavor changing neutral current (FCNC) processes is expected to come from gluino exchange, since the quark-squark-gluino vertex is proportional to g_s and involves both chiralities, generating all the operators in Eq. (1). Therefore, we study the constraints on the off-diagonal mass terms connecting up- and charm-type squarks of helicities A and B in the super-Cabibbo-Kobayashi-Maskawa basis, normalized to the average squark mass, denoted by $(\delta_{12}^u)_{AB}$. The bounds scale linearly with the average squark mass, up to logarithmic terms due to QCD evolution. For reference, we report the constraints obtained for gluino and average squark masses of 1 TeV. As above, we only quote the constraints obtained from the CP-violating part of the $\Delta C = 2$ amplitude, which correspond to bounds on the imaginary part of $(\delta_{12}^u)_{AB}^2$. A constraint on the real part could be obtained by making an educated guess on the size of the SM contribution; however, we prefer to stick to model-independent results in the present analysis.

We use the mass-insertion approximation for degenerate squarks at the next-to-leading order in QCD [26,39,40] (see Ref. [41] for the results of the SUSY matching in the mass-eigenstate basis). The bounds are reported in Table III (see Refs. [3,5,6,9,12,14,16,17,19,21] for previous analyses). Since there is no SM contribution, the bounds on the SUSY $(\delta_{12}^u)_{AB}$ are invariant under the exchange of chiralities.

We cannot compare directly the present bounds in Table III with our previous results [5] which reported bounds on the absolute values of the $(\delta_{12}^u)_{AB}$ using an estimate of the long-distance contributions. For the sake of comparison, we have checked that following the same procedure as in Ref. [5] we obtain bounds stronger by a factor from 3 to 5.

TABLE III. Upper bounds at 95% probability on $\sqrt{|\mathrm{Im}(\delta_{12}^u)_{AB}^2|}$ for squark and gluino masses equal to 1 TeV. The three bounds are respectively obtained assuming: (i) a dominant LL (or RR) mass insertion, (ii) a dominant LR (or RL) mass insertion, (iii) $(\delta_{12}^u)_{LL} = (\delta_{12}^u)_{RR}$.

$\sqrt{\lvert\mathrm{Im}(\delta_{12}^u)_{LL,RR}^2\rvert}$	$\sqrt{\lvert\mathrm{Im}(\delta_{12}^u)_{LR,RL}^2\rvert}$	$\sqrt{\lvert\mathrm{Im}(\delta_{12}^u)_{LL=RR}^2\rvert}$
0.019	0.0025	0.0011

TABLE IV. Simulation details for correlator computation at four values of the inverse gauge coupling $\beta = 3.80$, 3.90, 4.05 and 4.20. The quantities $a\mu_\ell$ and $a\mu_c$ stand for light and charmlike bare valence quark mass values respectively, expressed in lattice units.

β	$a^{-4}(L^3 \times T)$	$a\mu_\ell = a\mu_{\rm sea}$	$a\mu_c$
3.80	$24^3 \times 48$	0.0080, 0.0110	0.1982, 0.2331, 0.2742
$a \sim 0.098$ fm			
3.90	$24^3 \times 48$	0.0040, 0.0064, 0.0085, 0.0100	0.1828, 0.2150, 0.2529
$a \sim 0.085$ fm	$32^3 \times 64$	0.0030, 0.0040	
4.05	$32^3 \times 64$	0.0030, 0.0060, 0.0080	0.1572, 0.1849, 0.2175
$a \sim 0.067$ fm			
4.20	$32^3 \times 64$	0.0065	0.13315, 0.1566, 0.1842
$a \sim 0.054$ fm	$48^3 \times 96$	0.0020	

III. LATTICE SETUP AND SIMULATION DETAILS

The $N_f = 2$ gauge configuration ensembles employed in the present analysis have been generated by the ETM collaboration. The four values of the simulated lattice spacing lie in the interval [0.05, 0.1] fm. Dynamical quark simulations have been performed using the tree-level improved Symanzik gauge action [42] and the Wilson twisted mass action [43] tuned to maximal twist [44]. More details on the action and our $N_f = 2$ gauge ensembles can be found in Refs. [23,24,45,46]. We stress that the use of maximally twisted fermionic action offers the advantage of automatic $\mathrm{O}(a)$ improvement for all the interesting physical observables computed on the lattice [44].

For the evaluation of the four-fermion matrix elements on the lattice we use a mixed fermionic action setup where we adopt different regularizations for sea and valence quarks as proposed in Ref. [47]. This particular setup offers the advantage that one can compute matrix elements that are at the same time $\mathrm{O}(a)$ improved and free of wrong chirality mixing effects [48]. These two properties have already proved to be very beneficial in the study of neutral K- and B-meson oscillations [27,28,49–52].

We have computed 2- and 3-point correlation functions with valence quark masses ranging from the light sea quark mass up to around the physical charm quark mass. Simulation details are given in Table IV, where μ_ℓ and μ_c indicate the bare light and charmlike valence quark masses respectively. The values of the light valence quark mass are set equal to the light sea ones, $a\mu_\ell = a\mu_{\rm sea}$, and they correspond to light pseudoscalar mesons in the range 280–500 MeV.

Renormalized quark masses are obtained from the bare ones using the renormalization constant $Z_\mu = Z_P^{-1}$ [43,47], whose values have been computed in [28,53] using RI-MOM techniques. The physical values for the light and charm quark mass are $\bar{m}_{u/d}(2\ \mathrm{GeV}) = 3.6(2)$ MeV and $\bar{m}_c(m_c) = 1.28(4)$ GeV, taken from Ref. [24].

We have computed 2- and 3- point correlation functions by employing smearing techniques on a set of 100–240 independent gauge configurations for each ensemble and evaluated statistical errors using a bootstrap method.[1] Smeared interpolating operators become mandatory in the presence of relativistic heavy (charmlike and heavier) quarks. Smearing turns out to reduce the coupling of the interpolating field with the excited states, thus increasing its projection onto the lowest energy eigenstate. The usual drawback, i.e. the increase of the gauge noise due to fluctuations of the links entering in the smeared fields, is controlled by replacing thin gauge links with array processor experiment (APE) smeared ones. With this technical improvement heavy-light meson masses and matrix elements can be extracted at relatively small temporal separations while keeping noise-to-signal ratio under control. We employed Gaussian smearing [54,55] for heavy-light meson interpolating fields at the source and/or the sink. The smeared field is of the form

$$\Phi^{\rm S} = (1 + 6\kappa_{\rm G})^{-N_{\rm G}}(1 + \kappa_{\rm G} a^2 \nabla^2_{\rm APE})^{N_{\rm G}} \Phi^{\rm L}, \qquad (5)$$

where $\Phi^{\rm L}$ is a standard local source and $\nabla_{\rm APE}$ is the lattice covariant derivative with APE smeared gauge links characterized by the parameters $\alpha_{\rm APE} = 0.5$ and $N_{\rm APE} = 20$. We have taken $\kappa_{\rm G} = 4$ and $N_{\rm G} = 30$. We have noticed that in practice a better signal to noise ratio is found when the source, rather than the sink, is smeared. Thus 2-point smeared-local correlation functions yield better improved plateaux for the lowest energy mass state than local-smeared or smeared-smeared ones. In a recent paper [28] ETMC investigated optimized interpolating operators for both three- and two-point correlation functions both of which enter in the computation of the bag parameters. It has been found out that within the statistical uncertainty (which is at the level of 1% or less) no difference can be seen between the optimized and the simple smeared interpolating fields. In the present paper we use the same lattice data as those in Ref. [28]. For this reason we are confident that excited states are well suppressed for our plateau choices.

[1] The bootstrap method also serves the purpose of taking into account correlations over different time slices.

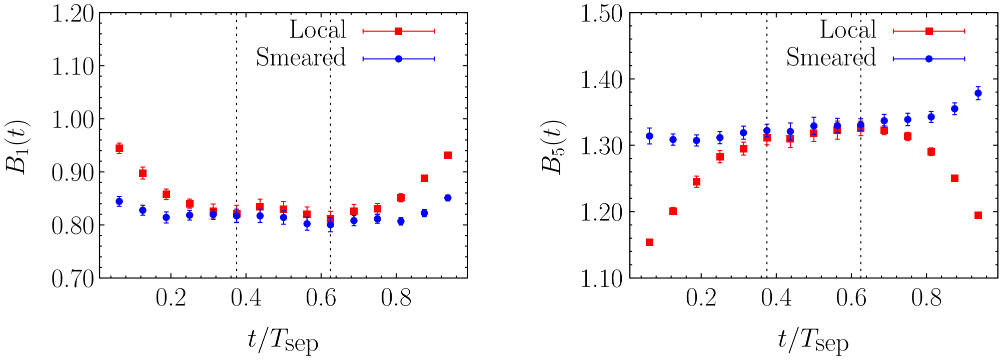

FIG. 2 (color online). $B_1(t)$ (left) and $B_5(t)$ (right) using either smeared or local sources at $\beta = 3.80$ and $(a\mu_\ell, a\mu_c) = (0.0080, 0.2331)$ on a $24^3 \times 48$ lattice. The dotted vertical lines delimit the plateau regions.

In Fig. 2 we show (time-dependent estimators of) the B_1 and B_5 bare bag parameters at $\beta = 3.80$ for the smallest light quark mass and a charmlike quark around the physical charm, and compare the cases of smeared versus local quark sources in both the heavy-light meson interpolating fields.

The bare bag parameters can be evaluated from ratios of 3-point, $C_{3;i}(x_0)$, and two 2-point, $C_2(x_0)$ and $C_2'(x_0)$, correlation functions [for more details see the discussion that leads to Eqs. (4.10)–(4.13) of Ref. [27]]:

$$\xi_i B_i(x_0) = \frac{C_{3;i}(x_0)}{C_2(x_0) C_2'(x_0)}, \quad i = 1, \ldots, 5. \tag{6}$$

To improve the signal-to-noise ratio a sum was performed over the spatial position of the four-fermion operator in $C_{3;i}(x_0)$, and for each gauge configuration the time slice y_0 was randomly chosen. An important reduction of statistical fluctuations comes also from summing over the spatial position of both (local or smeared) meson interpolating fields. These spatial sums were implemented at a reasonably low computational cost by means of the stochastic technique discussed in Sec. 2.2 of Ref. [49].

The plateau of the ratio (6), for large source time separation $T_{\rm sep}$, provides an estimate of the (bare) B_i ($i = 1, \ldots, 5$) bag parameter multiplied by the corresponding factor ξ_i in Eq. (3). By employing smeared interpolating operators for the meson sources we are able to reduce the source time separation, $T_{\rm sep}$. The latter, in order to lead to safe plateau signals, turns out to be less than half of the lattice time extension: $T_{\rm sep}/a = \{16, 18, 22, 28\}$ for $\beta = \{3.80, 3.90, 4.05, 4.22\}$, respectively.

For illustration, in Fig. 3 we show an exploratory test of the effect of locating the source and sink fields at different time slices. We observe that for both choices, $T_{\rm sep} = 16$ and $T_{\rm sep} = 24$, there is a visible plateau. Choosing $T_{\rm sep} = 16$, as in the present analysis, one obtains data that are more precise than in the $T_{\rm sep} = 24$ case.

IV. RESULTS FOR THE BAG PARAMETERS AT THE PHYSICAL POINT

The bag parameters are renormalized nonperturbatively by using the RI-MOM [56] renormalization constants computed in Ref. [27].

For all bag parameters B_i the results are first interpolated to the physical value of the charm quark mass [24]. Since

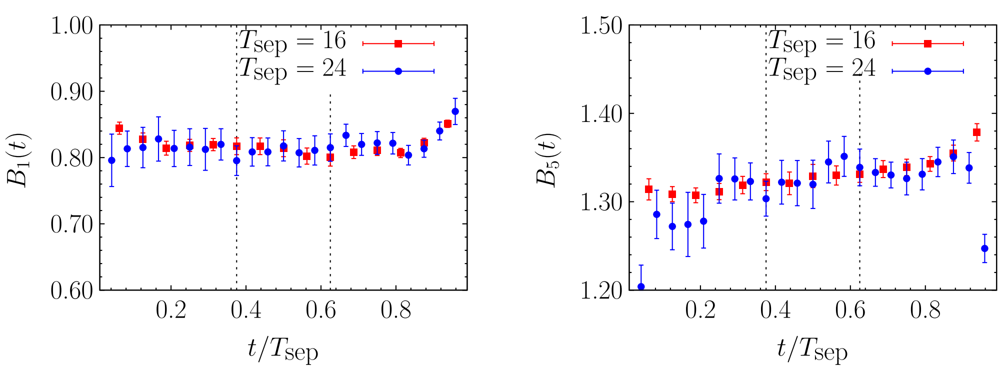

FIG. 3 (color online). $B_1(t)$ (left) and $B_5(t)$ (right) at $\beta = 3.80$ and $(a\mu_\ell, a\mu_c) = (0.0080, 0.2331)$ on a $24^3 \times 48$ lattice for smeared sources and sink located at two different time distances ($T_{\rm sep}$).

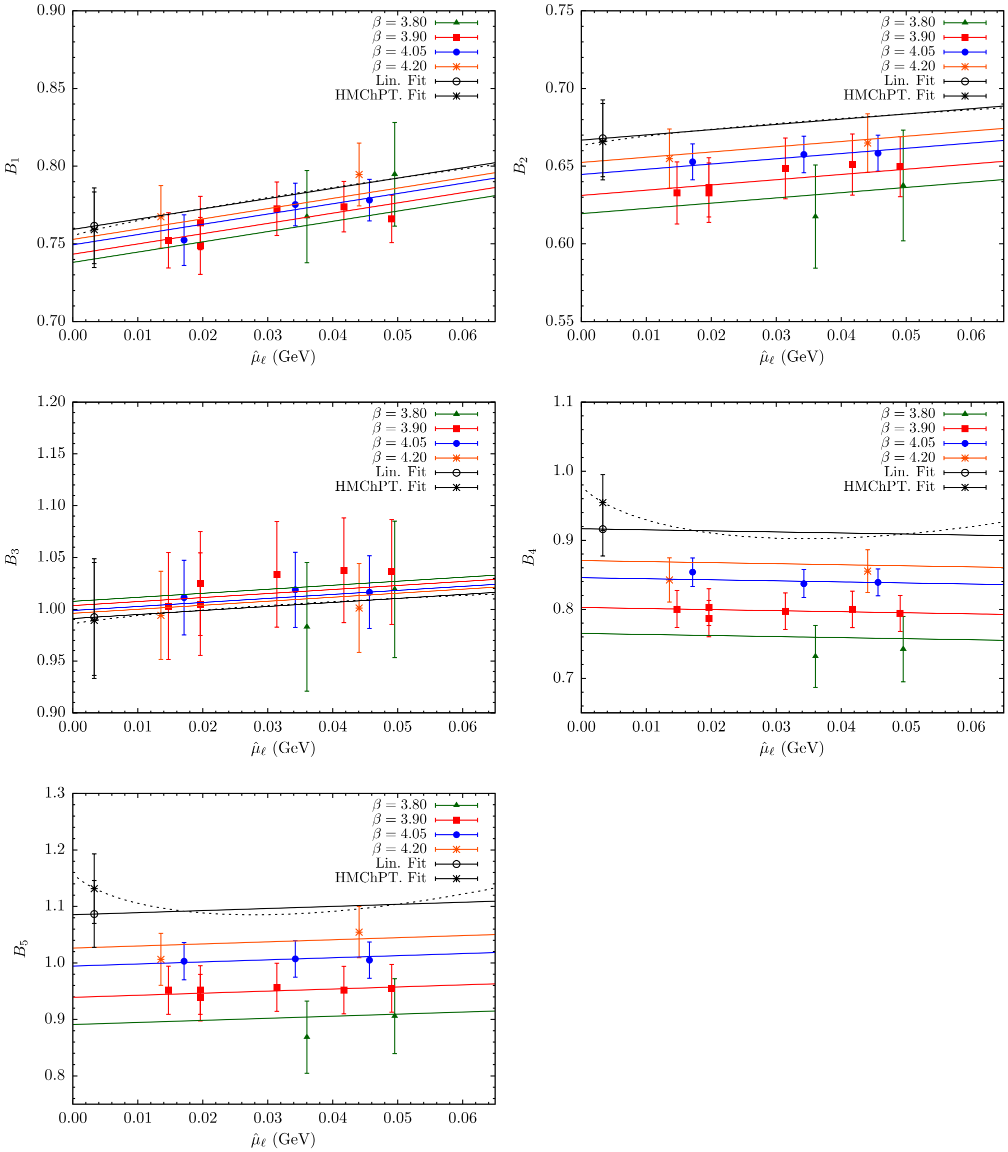

FIG. 4 (color online). Combined chiral and continuum extrapolation for the B_i parameters ($i = 1, 2, 3, 4, 5$) renormalized in the $\overline{\mathrm{MS}}$ scheme of Ref. [26] at 3 GeV. Solid lines represent the linear chiral fit with the continuum curve displayed in black. The dashed black line represents the continuum curve in the case of the HMChPT ansatz. Open circles and stars stand for the results at the physical point corresponding to the linear and HMChPT fit, respectively.

we have simulated three points around the physical charm quark mass, the interpolation is under very good control and a linear interpolation turns out to describe correctly the smooth mass dependence.

Continuum and chiral extrapolation are carried out in a combined way. For all bag parameters, we have tried out a linear fit in the light quark mass, $\bar{\mu}_\ell$, renormalized in $\overline{\mathrm{MS}}$ at 2 GeV,

$$B_i = A_i + B_i\bar{\mu}_\ell + D_i a^2, \tag{7}$$

a quadratic fit

$$B_i = A_i' + B_i'\bar{\mu}_\ell + C_i'\bar{\mu}_\ell^2 + D_i' a^2, \tag{8}$$

and a heavy meson chiral perturbation theory (HMChPT) fit ansatz [57],

$$\begin{aligned} B_1 &= B_1^\chi\left[1 + b_1\bar{\mu}_\ell - \frac{(1-3\hat{g}^2)}{2}\frac{2B_0\bar{\mu}_\ell}{16\pi^2 f_0^2}\log\frac{2B_0\bar{\mu}_\ell}{16\pi^2 f_0^2}\right] + \hat{D}_1 a^2, \\ B_i &= B_i^\chi\left[1 + b_i\bar{\mu}_\ell \mp \frac{(1\mp 3\hat{g}^2 Y)}{2}\frac{2B_0\bar{\mu}_\ell}{16\pi^2 f_0^2}\log\frac{2B_0\bar{\mu}_\ell}{16\pi^2 f_0^2}\right] + \hat{D}_i a^2, \end{aligned} \tag{9}$$

TABLE V. Bare $\xi_i B_i$ at each combination of the quark mass pair $(a\mu_l, a\mu_c)$ at $\beta = 3.80$ and $24^3 \times 48$ volume.

$\beta = 3.80$ $L^3 \times T = 24^3 \times 48$						
$a\mu_\ell = a\mu_{\rm sea}$	$a\mu_c$	$\xi_1 B_1$	$\xi_2 B_2$	$\xi_3 B_3$	$\xi_4 B_4$	$\xi_5 B_5$
0.0080	0.1982	2.126(30)	1.285(09)	0.289(03)	2.120(10)	0.860(06)
	0.2331	2.160(32)	1.307(09)	0.291(03)	2.135(11)	0.884(07)
	0.2742	2.193(35)	1.329(10)	0.291(03)	2.148(12)	0.909(08)
0.0110	0.1982	2.196(43)	1.326(24)	0.299(05)	2.153(35)	0.884(15)
	0.2331	2.236(44)	1.349(24)	0.301(05)	2.168(36)	0.910(15)
	0.2742	2.277(45)	1.373(24)	0.303(05)	2.181(37)	0.936(16)

TABLE VI. The same as in Table V but for $\beta = 3.90$ and $24^3 \times 48$ volume.

$\beta = 3.90$ $L^3 \times T = 24^3 \times 48$						
$a\mu_\ell = a\mu_{\rm sea}$	$a\mu_c$	$\xi_1 B_1$	$\xi_2 B_2$	$\xi_3 B_3$	$\xi_4 B_4$	$\xi_5 B_5$
0.0040	0.1828	2.089(28)	1.245(07)	0.284(02)	2.169(14)	0.883(08)
	0.2150	2.125(31)	1.269(07)	0.287(03)	2.186(15)	0.910(08)
	0.2529	2.157(34)	1.292(08)	0.289(03)	2.202(16)	0.938(10)
0.0064	0.1828	2.152(24)	1.269(08)	0.288(02)	2.159(16)	0.884(07)
	0.2150	2.192(26)	1.293(08)	0.290(02)	2.171(16)	0.910(07)
	0.2529	2.231(28)	1.317(08)	0.291(03)	2.182(16)	0.936(07)
0.0085	0.1828	2.155(18)	1.274(06)	0.289(01)	2.160(14)	0.881(07)
	0.2150	2.196(20)	1.298(07)	0.291(02)	2.178(15)	0.908(07)
	0.2529	2.235(21)	1.322(07)	0.293(02)	2.194(16)	0.937(08)
0.0100	0.1828	2.136(12)	1.273(05)	0.288(02)	2.148(11)	0.880(05)
	0.2150	2.173(12)	1.295(06)	0.291(02)	2.163(12)	0.907(06)
	0.2529	2.209(13)	1.318(06)	0.292(02)	2.176(13)	0.934(06)

where the sign in front of the logarithmic term is minus for $i = 2$ and plus for $i = 4, 5$. We take the HMChPT based estimate $Y = 1$ from Ref. [57] and $\hat{g} = 0.53(4)$ from the $(N_f = 2)$ lattice measurement of the $g_{D^*D\pi}$ coupling [58]. We observe that the contribution of the $\hat{g}$ uncertainty to the error of the chiral fit is less than 0.3% and that of the uncertainties due to B_0 and f_0 is less than 0.1%. In HQET the bag parameter B_3 is related to the bag parameters B_1 and B_2. For $Y = 1$, which is the only case considered in this paper, the chiral expansion for B_3 is similar to the one of B_2 with the same chiral log.

In Fig. 4 we show the combined chiral and continuum fit for the renormalized B_i in the $\overline{\rm MS}$ scheme of Ref. [26] at 3 GeV. Our final results for the B_i bag parameters in the $\overline{\rm MS}$ and RI-MOM scheme at 3 GeV, obtained by averaging the estimates from the three chiral fits discussed above, are collected in Table I. The quadratic fit results turn out to be very close to those of the linear fit. The half of the difference between the two more distant results, i.e. between the results of the linear and HMChPT fits, has been included as a systematic error, added in quadrature to the statistical one. In performing the combined chiral and continuum fits statistical errors of the (bare) bag parameters and statistical uncertainties of the renormalization constants of two- and four-fermion operators have been included and treated altogether employing the bootstrap procedure. We note that statistical errors of the renormalization constants represent a significant source of uncertainty. Their contribution in the final error budget lies between 2% and 3.5%, depending on B_i. The largest one is noted for B_3. Moreover, we have added in quadrature the systematic error owed to the way that discretization effects have been estimated in computing the renormalization constants.[2] This systematic uncertainty varies from 0.5% to 2.5%.

ACKNOWLEDGMENTS

We acknowledge the computer time available on the Altix system at the HLRN supercomputing service in Berlin under the project "B-physics from lattice QCD simulations." Part of this work has been completed thanks to allocation of CPU time on BlueGene/Q–Fermi based on the agreement between INFN and CINECA within the specific initiative INFN-RM123. The research leading to these results has received funding from the European Research Council under the European Union's Seventh Framework Programme (FP/2007-2013)/ERC Grant

[2]More details on the RI-MOM computation of the renormalization constants and the two possible ways to work out estimates concerning discretization errors can be found in Refs. [27,53].

Agreements No. 279972 “NPFlavour” and No. 267985 “DaMeSyFla.” F. S. has received funding from the European Research Council under the European Union’s Seventh Framework Programme (FP7/2007-2013) ERC Grant Agreement No. 279757. We also thank MIUR (Italy) for partial support under the Contract No. PRIN10-11.

APPENDIX: LATTICE DATA FOR THE BARE BAG PARAMETERS

In this Appendix, in Tables V,VI,VII,VIII,IX,X, we collect the results for the *bare* bag parameters, for all simulated values of β and combinations of quark masses.

TABLE VII. The same as in Table V but for $\beta = 3.90$ and $32^3 \times 64$ volume.

$\beta = 3.90$ $L^3 \times T = 32^3 \times 64$						
$a\mu_\ell = a\mu_{\rm sea}$	$a\mu_c$	$\xi_1 B_1$	$\xi_2 B_2$	$\xi_3 B_3$	$\xi_4 B_4$	$\xi_5 B_5$
0.0030	0.1828	2.099(28)	1.238(12)	0.279(04)	2.165(16)	0.881(07)
	0.2150	2.134(30)	1.262(13)	0.282(04)	2.179(17)	0.908(08)
	0.2529	2.168(32)	1.286(14)	0.284(05)	2.193(19)	0.937(09)
0.0040	0.1828	2.119(25)	1.239(06)	0.281(02)	2.128(16)	0.868(05)
	0.2150	2.165(26)	1.262(07)	0.282(02)	2.142(17)	0.895(05)
	0.2529	2.212(27)	1.285(07)	0.283(02)	2.155(18)	0.923(06)

TABLE VIII. The same as in Table V but for $\beta = 4.05$ and $32^3 \times 64$ volume.

$\beta = 4.05$ $L^3 \times T = 32^3 \times 64$						
$a\mu_\ell = a\mu_{\rm sea}$	$a\mu_c$	$\xi_1 B_1$	$\xi_2 B_2$	$\xi_3 B_3$	$\xi_4 B_4$	$\xi_5 B_5$
0.0030	0.1572	2.058(29)	1.213(08)	0.277(03)	2.183(16)	0.881(07)
	0.1849	2.088(32)	1.234(10)	0.279(03)	2.202(17)	0.910(07)
	0.2175	2.114(36)	1.255(12)	0.280(04)	2.219(19)	0.940(08)
0.0060	0.1572	2.115(23)	1.221(08)	0.279(03)	2.144(15)	0.875(07)
	0.1849	2.151(25)	1.243(09)	0.281(03)	2.160(16)	0.904(08)
	0.2175	2.185(28)	1.265(10)	0.282(04)	2.175(18)	0.933(09)
0.0080	0.1572	2.121(20)	1.223(08)	0.279(02)	2.149(11)	0.877(05)
	0.1849	2.158(22)	1.245(08)	0.280(02)	2.165(12)	0.904(06)
	0.2175	2.195(25)	1.266(09)	0.281(03)	2.179(12)	0.931(07)

TABLE IX. The same as in Table V but for $\beta = 4.20$ and $32^3 \times 64$ volume.

$\beta = 4.20$ $L^3 \times T = 32^3 \times 64$						
$a\mu_\ell = a\mu_{\rm sea}$	$a\mu_c$	$\xi_1 B_1$	$\xi_2 B_2$	$\xi_3 B_3$	$\xi_4 B_4$	$\xi_5 B_5$
0.0065	0.13315	2.128(32)	1.205(12)	0.278(04)	2.157(20)	0.878(10)
	0.1566	2.174(33)	1.229(13)	0.280(05)	2.178(20)	0.908(11)
	0.1842	2.220(33)	1.253(15)	0.282(05)	2.199(21)	0.940(12)

TABLE X. The same as in Table V but for $\beta = 4.20$ and $48^3 \times 96$ volume.

$\beta = 4.20$ $L^3 \times T = 48^3 \times 96$						
$a\mu_\ell = a\mu_{\rm sea}$	$a\mu_c$	$\xi_1 B_1$	$\xi_2 B_2$	$\xi_3 B_3$	$\xi_4 B_4$	$\xi_5 B_5$
0.0020	0.13315	2.068(33)	1.187(12)	0.275(04)	2.130(28)	0.853(12)
	0.1566	2.100(33)	1.211(13)	0.278(05)	2.143(29)	0.879(13)
	0.1842	2.131(34)	1.234(15)	0.280(06)	2.156(31)	0.905(14)

[1] B. Aubert *et al.* (*BABAR* Collaboration), Phys. Rev. Lett. **98**, 211802 (2007).
[2] M. Staric *et al.* (Belle Collaboration), Phys. Rev. Lett. **98**, 211803 (2007).
[3] F. Gabbiani, E. Gabrielli, A. Masiero, and L. Silvestrini, Nucl. Phys. **B477**, 321 (1996).
[4] G. Raz, Phys. Rev. D **66**, 057502 (2002).
[5] M. Ciuchini, E. Franco, D. Guadagnoli, V. Lubicz, M. Pierini, V. Porretti, and L. Silvestrini, Phys. Lett. B **655**, 162 (2007).
[6] Y. Nir, J. High Energy Phys. 05 (2007) 102.
[7] M. Blanke, A. J. Buras, S. Recksiegel, C. Tarantino, and S. Uhlig, Phys. Lett. B **657**, 81 (2007).
[8] X.-G. He and G. Valencia, Phys. Lett. B **651**, 135 (2007).
[9] E. Golowich, J. Hewett, S. Pakvasa, and A. A. Petrov, Phys. Rev. D **76**, 095009 (2007).
[10] M. Bona *et al.* (UTfit Collaboration), J. High Energy Phys. 03 (2008) 049.
[11] B. Dutta and Y. Mimura, Phys. Rev. D **77**, 051701 (2008).
[12] G. Hiller, Y. Hochberg, and Y. Nir, J. High Energy Phys. 03 (2009) 115.
[13] C.-H. Chen, Phys. Lett. B **680**, 133 (2009).
[14] O. Gedalia, Y. Grossman, Y. Nir, and G. Perez, Phys. Rev. D **80**, 055024 (2009).
[15] A. L. Kagan and M. D. Sokoloff, Phys. Rev. D **80**, 076008 (2009).
[16] W. Altmannshofer, A. J. Buras, S. Gori, P. Paradisi, and D. M. Straub, Nucl. Phys. **B830**, 17 (2010).
[17] W. Altmannshofer, A. J. Buras, and P. Paradisi, Phys. Lett. B **688**, 202 (2010).
[18] G. Isidori, Y. Nir, and G. Perez, Annu. Rev. Nucl. Part. Sci. **60**, 355 (2010).
[19] A. Crivellin and M. Davidkov, Phys. Rev. D **81**, 095004 (2010).
[20] D. Guadagnoli and R. N. Mohapatra, Phys. Lett. B **694**, 386 (2011).
[21] L. Calibbi, Z. Lalak, S. Pokorski, and R. Ziegler, J. High Energy Phys. 06 (2012) 018.
[22] A. Bevan *et al.* (UTfit Collaboration), J. High Energy Phys. 10 (2012) 068.
[23] R. Baron *et al.* (ETM Collaboration), J. High Energy Phys. 08 (2010) 097.
[24] B. Blossier, P. Dimopoulos, R. Frezzotti, V. Lubicz, M. Petschlies, F. Sanfilippo, S. Simula, and C. Tarantino (ETM Collaboration), Phys. Rev. D **82**, 114513 (2010).
[25] N. Carrasco, V. Lubicz, and L. Silvestrini, arXiv:1312.6691.
[26] A. Buras, M. Misiak, and J. Urban, Nucl. Phys. **B586**, 397 (2000).
[27] V. Bertone *et al.* (ETM Collaboration), J. High Energy Phys. 03 (2013) 089.
[28] N. Carrasco, M. Ciuchini, P. Dimopoulos, R. Frezzotti, V. Gimenez *et al.*, J. High Energy Phys. 03 (2014) 016.
[29] A. Bevan *et al.* (UTfitCollaboration), J. High Energy Phys. 03 (2014) 123.
[30] Z. Ligeti, M. Papucci, G. Perez, and J. Zupan, Phys. Rev. Lett. **105**, 131601 (2010).
[31] A. J. Buras, K. Gemmler, and G. Isidori, Nucl. Phys. **B843**, 107 (2011).
[32] A. Lenz, U. Nierste, J. Charles, S. Descotes-Genon, A. Jantsch, C. Kaufhold, H. Lacker, S. Monteil, V. Niess, and S. T'Jampens, Phys. Rev. D **83**, 036004 (2011).
[33] E. Lunghi and A. Soni, Phys. Lett. B **697**, 323 (2011).
[34] Y. Adachi, N. Kurahashi, N. Maru, and K. Tanabe, Phys. Rev. D **85**, 096001 (2012).
[35] L. Calibbi, Z. Lalak, S. Pokorski, and R. Ziegler, J. High Energy Phys. 07 (2012) 004.
[36] B. Keren-Zur, P. Lodone, M. Nardecchia, D. Pappadopulo, R. Rattazzi, and L. Vecchi, Nucl. Phys. **B867**, 394 (2013).
[37] F. Mescia and J. Virto, Phys. Rev. D **86**, 095004 (2012).
[38] A. J. Buras, F. De Fazio, J. Girrbach, and M. V. Carlucci, J. High Energy Phys. 02 (2013) 023.
[39] M. Ciuchini, E. Franco, V. Lubicz, G. Martinelli, I. Scimemi, and L. Silvestrini, Nucl. Phys. **B523**, 501 (1998).
[40] M. Ciuchini, E. Franco, D. Guadagnoli, V. Lubicz, V. Porretti, and L. Silvestrini, J. High Energy Phys. 09 (2006) 013.
[41] J. Virto, J. High Energy Phys. 11 (2009) 055.
[42] P. Weisz, Nucl. Phys. **B212**, 1 (1983).
[43] R. Frezzotti, P. A. Grassi, S. Sint, and P. Weisz (Alpha Collaboration), J. High Energy Phys. 08 (2001) 058.
[44] R. Frezzotti and G. C. Rossi, J. High Energy Phys. 08 (2004) 007.
[45] P. Boucaud *et al.* (ETM Collaboration), Phys. Lett. B **650**, 304 (2007).
[46] P. Boucaud *et al.* (ETM Collaboration), Comput. Phys. Commun. **179**, 695 (2008).
[47] R. Frezzotti and G. C. Rossi, J. High Energy Phys. 10 (2004) 070.
[48] M. Bochicchio, L. Maiani, G. Martinelli, G. Rossi, and M. Testa, Nucl. Phys. **B262**, 331 (1985).
[49] M. Constantinou *et al.* (ETM Collaboration), Phys. Rev. D **83**, 014505 (2011).
[50] P. Dimopoulos, H. Simma, and A. Vladikas, J. High Energy Phys. 07 (2009) 007.
[51] N. Carrasco, V. Gimenez, P. Dimopoulos, R. Frezzotti, D. Palao *et al.* (ETM Collaboration), Proc. Sci., LATTICE2011 (**2011**) 276.
[52] N. Carrasco *et al.* (ETM Collaboration), arXiv:1310.5461.
[53] M. Constantinou *et al.* (ETM Collaboration), J. High Energy Phys. 08 (2010) 068.
[54] S. Gusken, Nucl. Phys. B, Proc. Suppl. **17**, 361 (1990).
[55] K. Jansen, C. Michael, A. Shindler, and M. Wagner (ETM Collaboration), J. High Energy Phys. 12 (2008) 058.
[56] G. Martinelli, C. Pittori, C. T. Sachrajda, M. Testa, and A. Vladikas, Nucl. Phys. **B445**, 81 (1995).
[57] D. Becirevic, S. Fajfer, and J. F. Kamenik, J. High Energy Phys. 06 (2007) 003.
[58] D. Becirevic and F. Sanfilippo, Phys. Lett. B **721**, 94 (2013).